Int. J. Environ. Sci. Technol. (2014) 11:159–168
DOI 10.1007/s13762-013-0370-5

ORIGINAL PAPER

Characterization of activated carbon obtained from Saudi Arabian fly ash

A. Mofarrah · T. Husain · C. Bottaro

Received: 10 September 2011 / Revised: 2 January 2012 / Accepted: 22 January 2013 / Published online: 25 September 2013

Abstract This study investigated the potential application of heavy oil burning fly ash as a precursor to prepare activated carbon. The raw fly ash obtained from a power plant is cleaned by nitric acid/hydrochloric acid and activated at 550–800 °C with hold times of 30 and 60 min to obtain fly ash activated carbon. The phosphoric acid is used as a chemical agent to improve the surface characteristics of the cleaned fly ash. The effects of process variables such as amount of chemical reagents, activation time and temperature were investigated according to two-levels full factorial design. The resultant activated carbons were characterized in terms of Brunauer, Emmett and Teller surface area and total and pore volume. The maximum specific surface area was found of 148.30 m^2/g at 800 °C temperatures with 60 min holding time. The test showed that the surface area and pore volumes of the material are also significantly enhanced by the activation process.

Keywords Chemical activation · Factorial design · Surface area · Unburned carbon

Introduction

During the combustion of fuel oil in boilers, oil drops are heated and burned with oxygen and then depleted; at the same time, the impurities, such as sulfur, vanadium and nickel, within the fuel oil also undergo transformations and react with gaseous hydrocarbons to form particulates known as ash (Turner and Steve 2009). Burning heavy fuel oil yields about 3 kilogram (kg) of ash per kiloliter of oil (Tsai and Tsai 1997), and most of the ashes (approximately 90 %) are fly ash (FA), which is collected by electrostatic precipitators or cyclones, for final disposal or re-use (Hsieh and Tsai 2003). Heavy oil fly ash (HOFA) consists of inorganic substances such as silicon dioxide (SiO_2), iron oxide (Fe_2O_3), aluminum oxide (Al_2O_3) and 70–80 % unburned carbon (Kwon et al. 2005). The HOFA contains a good amount of valuable metallic compounds such as vanadium (V) (20–30 %), nickel (Ni) (0.8–6 %), arsenic (As), cadmium (Cd), mercury (Hg), chromium (Cr) and copper (Cu) (Mofarrah et al. 2011; Zhang et al. 1995; Lozano and Juan 2001; Hwang et al. 1996). Worldwide several million tonnes of HOFA are generated each year, and only a small portion of these ashes is re-used for productive purposes (Mõtlep et al. 2010). The remaining amount of HOFA must be disposed either into the landfills or waste containment facilities. HOFA is an environmental concern, indeed poor management and uncontrolled disposal may cause a dispersion of fine particles containing pollutants, which are hazardous to health (Fernandez et al. 2003; Mohapatra and Rao 2001). Exposure to HOFA has negative biological effects (e.g., lung injury) as well as effects on the environment (Jiang et al. 2000; Andrew et al. 2002; Onundi et al. 2011). Due to low density (0.25 g/cm^3) and fine particulate size, it has potential to travel large distances and may pose negative effects on plants and animals in a variety of ways. Nowadays, management of FA waste has become an emerging issue in different areas of the world. The characteristics study showed that HOFA contained a high percentage of unburned carbon, which can

A. Mofarrah (✉) · T. Husain
Department of Civil Engineering, Memorial University of Newfoundland, St. John's, NL A1B 3X5, Canada
e-mail: abdullah.mofarrah@gmail.com

C. Bottaro
Department of Chemistry, Memorial University of Newfoundland, St. John's, NL A1B 3X7, Canada

be used as alternative raw material for activated carbon (AC) preparation. AC is defined as carbonaceous material having high porosity and internal surface area (Cuhadaroglu and Uygun 2008). High surface area, high surface reactivity, suitable pore distribution and mechanical strength are the desired properties for an AC. Both starting material and preparation methods influence the final properties of AC. The commercial AC has internal surface areas in the range of 500–1,500 m^2/g; and the higher surface area is preferred as a better adsorbent (Caramuscio et al. 2003). Generally, two production processes, namely physical and chemical activation, are used in AC production. Physical activation consists of pyrolysis of the carbonaceous matrix under inert atmosphere followed by gasification of the resulting char in the presence of some mildly oxidizing gases such as CO_2 or steam (Wigmans 1989). Chemical activation consists of pyrolysis of the precursor in presence of chemical agents that are normally alkali and alkaline earth and some acids such as potassium hydroxide (KOH), potassium carbonate (K_2CO_3), sodium hydroxide (NaOH), sodium carbonate (Na_2CO_3), aluminum chloride ($AlCl_3$), zinc chloride ($ZnCl_2$), magnesium chloride ($MgCl_2$) and phosphoric acid (H_3PO_4) (Ahmadpour and Do 1996).

Commercially, AC is produced by pyrolysis and activation of materials with high carbon content such as wood, bamboo, coconut shell, petroleum coke and bituminous coals. Use of such valuable material increases the production cost of AC. On the other hand, re-uses of industrial waste like FA as raw material for AC production will simultaneously eliminate the environmental pollution and reduce the cost of AC production. This potentiality encourages the present study to produce AC by using HOFA. For this study, the FA samples were collected directly from the electrostatic precipitator (ESP) at a Power Plant (PP) in Saudi Arabia, and the research study was conducted at Memorial University of Newfoundland, Canada in 2011.

Materials and methods

For this study, HOFA samples were collected directly from the electrostatic precipitator (ESP) at a Power Plant (PP) in Saudi Arabia, which uses high sulfur content (1.5–3 %) heavy fuel oil. The physical properties of the samples, such as bulk density, specific gravity, loss on ignition (IOL) and moisture content, were analyzed following the testing method described by Wesche and others (Wesche et al. 1989). The raw HOFA is treated by several washing and leaching processes to remove the impurities. The suggested chemicals for the washing and leaching process are 1 M H_2SO_4 (Otterturn and Standell 1979), 28 % nitric acid (HNO_3), or 15 % hydrochloric acid (HCl) (Davini 2002), H_2O (Kaneko et al. 1992). For this study, the raw HOFA was treated with an aqueous acid solution at a ratio of 10 g of HOFA per 50 ml of nitric acid (28 % HNO_3) at 60 °C for 2 h as suggested by Hsieh and Tsai (2003). The mixture was continuously stirred by Phipps & Bird stirrer model 7,790–400 with 10 rpm over the test period. During the stirring process, a magnetic bar was immersed in the solution to capture impurities having magnetic properties.

After filtration, the residues were washed with distilled water several times to eliminate the NO_3^- ions. Subsequently, the filtrate residue was treated with 15 % HCl solution at a solid/liquid ratio of 1:5 at 60 °C for 1 h. The solution is then filtered to obtain the filtered cake. The filtered cake was rinsed repeatedly with distilled water to eliminate the chloride ions. Finally, the filtered cake was dried at 105 °C for 24 h to obtain the unburned carbon. Figure 1 shows the process diagram of unburned carbon recovery from HOFA.

The dried unburned carbon from washing processes was activated by mixing with H_3PO_4. The mixing ratio, temperature and activation times were varied according to a factorial design in Table 1.

The mixing of unburned carbon and chemicals was stirred continuously at 80 °C for 30 min and was dried at 100 °C for 24 h. After this process, the carbonization process was applied to the product obtained. The effect of temperature on carbonization was investigated by varying burning temperature between 550 and 800 °C. In carbonization process, generally the organic matter is converted into elemental carbon at high temperature, and it also

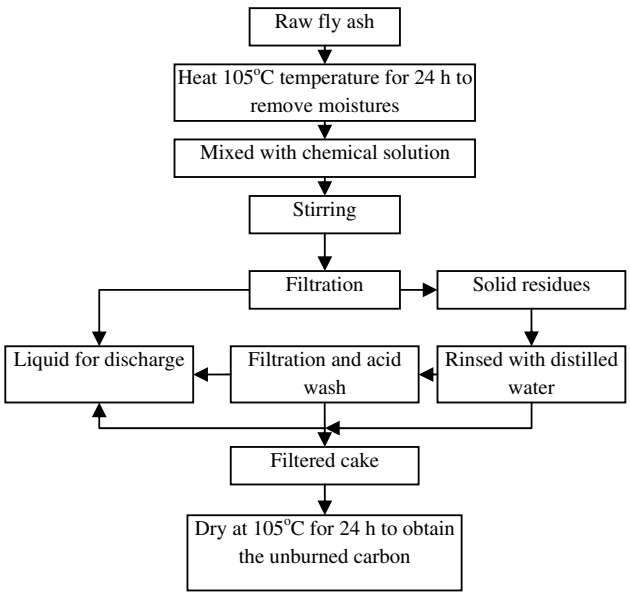

Fig. 1 Flow diagram to recover unburned carbon

Table 1 Design parameters for chemical activation process

Sample name	Coded values			Actual			Unburned carbon (g)
	A	B	C	Temperature (°C) A1	Heating time (min) B1	H_3PO_4 (ml) C1	
AC1	−	−	−	550	30	2	10
AC2	+	−	−	800	30	2	10
AC3	−	+	−	550	60	2	10
AC4	+	+	−	800	60	2	10
AC5	−	−	+	550	30	5	10
AC6	+	−	+	800	30	5	10
AC7	−	+	+	550	60	5	10
AC8	+	+	+	800	60	5	10

removes the volatiles matter from the material. At the end of activation process, the porosity of the carbonized matter is increased, which provides higher surface area of the produced AC.

For this study, the carbonization process was conducted in a programmable Lindberg/Blue M tube furnace (Fig. 2). This furnace provides the versatility and control accuracy to meet critical temperature required for the system. The furnace was programmed in such a way that heating rate was increased 5 °C/min until reaching the final temperature. It then remained at final temperature for 30 or 60 min, respectively, according to Table 1. At the end of this period, the furnace was left to cool at room temperature. During the heating period, a constant air flow of 5 ml/min was applied to the system to expedite the burning process. A similar approach was applied by Rahman et al. (2006) to produce activated charcoal from coconut shell.

The carbonized product was cleaned with 0.5 N HCl by mixing of 10 g of carbonized product to 250 ml acid at 85 °C for 30 min. The filtered cake was then rinsed with distilled water several times until the pH of the mixture exceeds 6. Finally, the fly ash activated carbon (FAC) was dried at 100 °C for 24 h, and characteristic properties were determined. This experiment was varied according to a two-level full factorial design (Montgomery 1997), where the impacts of the following three factors were studied based on the surface area (m^2/g) of the produced AC.

(a) Effect of temperature variation during the activation process
(b) Impact of reaction time
(c) Impact of impregnation ratio between chemical reagents (H_3PO_4) and precursor

An ultrahigh resolution scanning electron microscope (SEM) and inductively coupled plasma-mass atomic spectrometry (ICP-MS) were used to study the surface structures and qualitative chemical analysis of HOFA, respectively. Energy dispersive spectrometer (EDS) was used to analyze the carbon and sulfur contents in the fly ash.

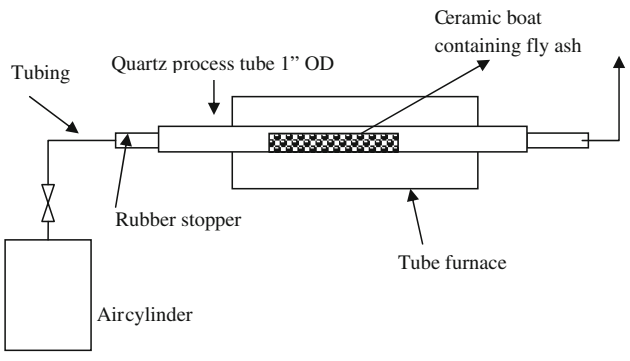

Fig. 2 The diagram of tube furnace for reaction experiment

Characterization of activated carbon

To characterize the ACs, researchers generally use some kind of gas phase adsorption measurements, leading to adsorption isotherms. These isotherms contain a wealth of information about the characteristics of AC. Different models are used to analyze the isotherms depending on adsorbates. The isotherms analysis involves a lot of uncertainty about the exact interpretation with gas and solid surface (Peter 2008). The first systematic attempt to interpret the adsorption isotherms of gas solid equilibrium was introduced by Brunauer, Deming, Deming and Teller (BDDT) (Brunauer et al. 1940). According to the BDDT classification, isotherms can be subdivided into six major categories (Gregg and Sing 1982; Sing et al. 1985;

Rouquerol et al. 1999). The shape of each isotherm depends on the type of adsorbent, the type of adsorbate and the intermolecular interaction between the gas and the adsorbent surface. The produced FACs were characterized by surface area and pore volume.

The surface area and porosity were measured by N_2 adsorption at 77 K using an automated adsorption apparatus BEL SOPR-MAX, BEL Japan Inc. The surface area (m^2/g) was measured from the application of the Brunauer, Emmett and Teller (BET) equation (Eq. 1), to the adsorption isotherms in the relative pressure range of 0.05–0.35, considering as 0.162 nm^2 the molecular area of N_2 at 77 K (Rodrı′guez-Reinoso 1989). Total pore volume, V_T, was obtained from N_2 adsorption isotherm at $p/p_0 = 0.99$.

$$\frac{1}{v\left(\frac{P_0}{P}-1\right)} = \frac{1}{v_m c} + \left(\frac{c-1}{v_m c}\right)\left(\frac{p}{p_0}\right) \quad (1)$$

$$v_m = \frac{1}{S+I} \quad (2)$$

$$c = 1 + \frac{S}{I} \quad (3)$$

$$\mathrm{SA_{BET}} = \frac{(v_m N A_{(N)})}{v} \quad (4)$$

$$\mathrm{S_{BET}} = \frac{\mathrm{SA_{BET}}}{a} \quad (5)$$

where v = volume adsorbed at standard temperature and pressure (STP); P and P_0 are the equilibrium and the saturation pressure of adsorbates at the temperature of adsorption; v_m = volume of gas (STP) required to form one monolayer; c = BET constant related to energy of adsorption; N = Avogadro's number, 6.02E + 23; $A_{(N)}$ = cross section of N_2 (0.162 nm^2); $\mathrm{SA_{BET}}$ = total BET surface area (m^2); $\mathrm{S_{BET}}$ = specific BET surface area (m^2/g); a = mass of adsorbent (in gm). The BET surface area can be calculated from the BET equation by plotting of $1/v\ [(P_0/P) - 1]$ on the y-axis and P/P_0 on the x-axis in the range of $0.05 < P/P_0 < 0.35$. The slope (S) and the y-intercept (I) of the line are used to calculate the monolayer adsorbed gas quantity v_m and the BET constant c.

There are many methods for calculation of pore-size distributions (Gregg and Sing 1982; Sing et al. 1985; Rouquerol et al. 1999). Among the others, the most common way of deriving the total micropore volume of an AC from any isotherm is by means of the Dubinin-Radushkevich (DR) equation (Gregg and Sing 1982). For this case, DR theory (Eq. 6) was applied on the N_2 isotherms to obtain the micropore volume.

$$W = W_0 \exp\left[-\left(\frac{BT}{\beta}\right)^2 \ln^2\left(\frac{P_0}{P}\right)\right] \quad (6)$$

where W = volume of the pores that has been filled at p/p_0 (cm^3/g); W_0 = total volume of the micropore (cm^3/g); B = structural constant related to the width of the Gaussian pore distribution (K^{-2}); T = temperature at which the isotherm has been taken (K); β = similarity constant, depending solely on the adsorbate; p_0/p = inverse of the relative pressure of the adsorbate. For a given adsorption process, validity of this equation can be established by plotting $\ln^2 (p_0/p)$ versus $\ln (W)$ at different temperatures. This plot yields a straight line (for at least some part of the plot) with an intercept of $\ln (W_0)$.

Statistical design of experiments

The statistical optimization technique using full factorial design of experiments is applied to determine the boundary conditions and maximum output of the produced ACs. The use of statistical design of experiments is advantageous as it allows one to obtain conditions through a relatively smaller number of systematic experiments. Using a proper design matrix, one can obtain a regression equation which highlights the effect of individual parameters and their relative importance in a given operation/process. The interactional effects of two or more variables can also be known, which is not possible in a classical experiment (Soylak et al. 2005). The principal steps of statistically designed experiments are determination of response variables, factors and factor levels, choice of the experimental design and statistical analysis of the data. In recent years, the most widely used experimental design to estimate main effects, as well as interaction effects, is the 2^n factorial design, where each variable is investigated at two levels (Singh et al. 2002).

For this study, the effects of three variables on the surface area development of unburned carbon were quantified based on a two-level full 2^3 factorial design of experiment. The experimental design involved 3 variables at 2 levels (i.e., low and high). In this case, the total number of experiments becomes 8. The variables and levels for the experimental along with actual and coded scales are given in Table 1. The higher level variable was designated as +1 and the lower level as −1. In Table 1, A1, B1 and C1 represent the level of temperature of sample burning, heating time of sample and the amount of H_3PO_4 added to fixed 10 g of unburned carbon, respectively, and A, B and C are the corresponding values in coded forms. The maximum and minimum levels are expressed in coded form as +1 and −1, respectively. The coded values are used to convert the absolute quantity

into a dimensionless factor, which is convenient for handling the experimental data.

Results and discussion

The chemical analysis of raw and cleaned HOFA is reported in Table 2. It shows that the HOFA is mainly composed of carbon (more than 85 %) with minor components such as vanadium (V), nickel (Ni), iron (Fe), copper (Cu), zinc (Zn) and tin (Sn). In order to prepare unburned carbon, the raw HOFA was cleaned by following several washing process (Fig. 1). The effect of washing leads to the removal of impurities such as metals and sulfur for the raw HOFA and increased pore volume and surface area. This happened due to extraction of mineral matters from the carbon structures. As shown in Table 2, the washing process noticeably reduced the metal concentrations; on the other hand, the pore volume and the surface area of the samples are increased.

SEM micrograph (Fig. 3a) shows that the particles characteristics of HOFA are mainly spherical in shape with few to several micrometers in size. The spherical particles are mostly porous in nature. The pores were individually situated and randomly located on the particle surface. Due to removal of impurities during the washing process, the

Table 2 Metals found in heavy oil fly ash

Metals	Raw HOFA (mg/kg)	Cleaned HOFA (mg/kg)
Arsenic (As)	2.239	0.006
Cadmium (Cd)	3.275	0.001
Cobalt (Co)	3.280	0.039
Chromium (Cr)	4.056	0.014
Copper(Cu)	170.40	0.40
Mercury (Hg)	0.245	ND
Nickel (Ni)	1,762.22	1.231
Lead (Pb)	10.995	0.014
Selenium (Se)	11.592	ND
Vanadium (V)	2,957.701	4.53
Zinc (Zn)	130.84	0.61
Carbon	85.20 %	91.23 %
Surface area	1.45	15.00
Total pore volume (cm^3/g)	0.0264	0.0412

ND not detectable

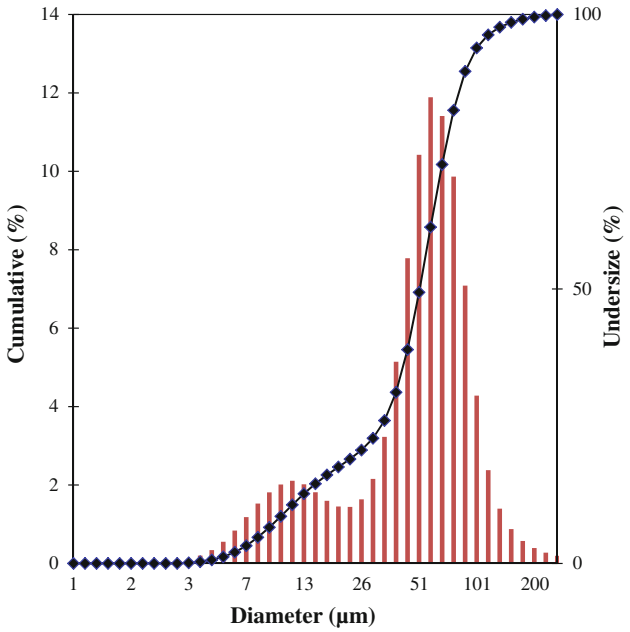

Fig. 4 Particles size distribution of fly ash

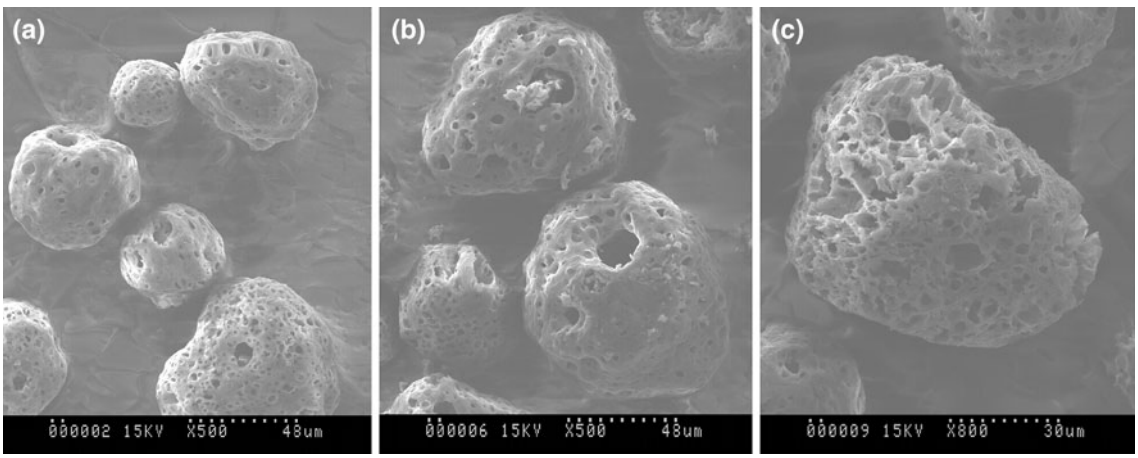

Fig. 3 SEM analysis of dry samples: **a** raw HOFA, **b** after washing treatment and **c** after heating at 900 °C

porosity of the particles is increased significantly (Fig. 3b). The carbonization process has significant influence on the particle's porosity development. As shown in Fig. 3c, the surface porosity of the HOFA is dramatically increased by chemical activation process. The laser scattering particles size analyzer confirmed that the mean diameter of the collected HOFA sample is 53.49 (μm) with standard deviation of 32.89 (μm). The particles size distribution of the fly ash is shown in Fig. 4.

Figure 5 shows the N_2-77 K adsorption isotherms for the chemically activated cleaned unburned carbon and raw HOFA. According to BDDT classification, these isotherms can be classified as Type I, concave to the P/P_o axis that is typical for microporous materials. However, the study isotherms do not reach the plateau at higher relative pressure, indicating the presence of meso- and macroporosity. The FAC prepared at higher temperature with maximum holding time and H_3PO_4 ratio showed higher adsorption of N_2 than other FAC. The surface area of the prepared FACs was estimated following the BET theory (Eq. 1–5) and reported in Table 3.

DR method (Eq. 6) was used to calculate the micropore volume of the produced FACs. In this case, the total pore volume was estimated at a partial pressure of 0.99 P/P_0 (STP) using the conversion factor of 0.001547, assuming the density of condensed N_2 in the pores is equal to the density of bulk liquid N_2 (Kruk and Jaroniec 2001).

For Example, the y-intercept of raw HOFA sample is 0.905 (Fig. 6); then, the micropore volume (V_{mc}) of the raw HOFA sample can be estimated as:

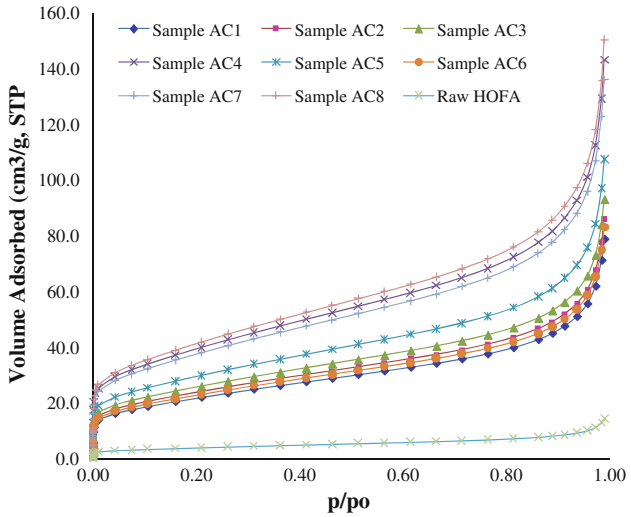

Fig. 5 N_2-77 K adsorption isotherms for prepared FAC and raw HOFA

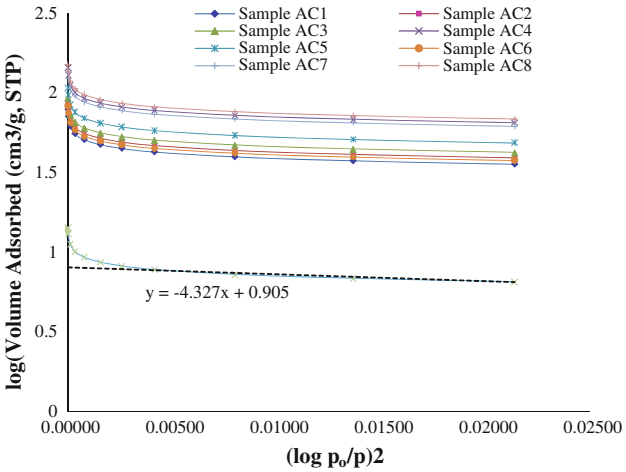

Fig. 6 Dubinin-Radushkevich plot for micropore volume estimation

Table 3 Textural properties of fly ash activated carbon

Sample	[a]BET Surface area (m^2/g)	[b]Total pore volume, V_T from $P/P_0 = 0.99$ (cm^3/g)	[c]Micropore volume V_{mc} (cm^3/g)	[d]Mesopore volume (cm^3/g)	[e]Mean pore diameter (nm)	% Yield of FAC
AC1	75.38	0.1219	0.05364	0.0683	6.4686	82.8
AC2	82.674	0.1329	0.05489	0.0780	6.4301	78.33
AC3	91.22	0.1440	0.058815	0.0852	6.5289	74.32
AC4	123.19	0.2215	0.097609	0.1239	7.1924	79.15
AC5	79.48	0.1285	0.061587	0.0669	6.4670	78.25
AC6	130.06	0.1662	0.057476	0.1087	4.8513	75.22
AC7	102.778	0.2105	0.086994	0.1235	8.1924	72.12
AC8	143.888	0.2326	0.109519	0.1231	6.4661	66.25
HOFA	1.45	0.0264	0.0124	0.0140	12.185	–

[a] Specific surface area A (m^2/g): BET equation ($P/P_0 = 0.05$–0.35)

[b] Total pore volume V_T (cm^3/g): Vads. ($P/P_0 = 0.99$) × 0.001547

[c] Micropore volume (cm^3/g): DR equation, $V_{intercept}$ × 0.001547

[d] Mesopore volume (cm^3/g):—$V_{mc} - V_T$

Table 4 Contribution of different parameters on surface area development

Parameters	Effects	% Contribution
A (Temperature)	32.65	45.74
B (Heating time)	23.28	23.26
C (H_3PO_4)	21.03	18.97
AB	3.89	0.65
AC	13.02	7.27
BC	−4.90	1.03
ABC	−8.45	3.06

Table 5 Experimental and predicted value of surface area (m^2/g) of FAC

Order	Experimental $_{BET}$ surface area (m^2/g)	Predicted $_{BET}$ surface area (m^2/g)
AC1	75.38	65.15
AC2	82.674	97.80
AC3	91.22	88.43
AC4	123.19	121.08
AC5	79.48	86.18
AC6	130.06	118.83
AC7	102.778	109.46
AC8	143.888	142.11

$$V_{mc} = 10^{0.905} \times 0.001547 = 0.0124 \quad (cm^3/g)$$

Table 3 shows the different properties of the FACs. It can be seen (Table 3) that the maximum surface area (i.e., 144 m^2/g for AC8) was achieved at 800 °C and 60 min of activation, which had the 5 ml H_3PO_4. The second height surface area was found 130 m^2/g (for AC6) at 800 °C and 30 min of activation, which had the 5 ml H_3PO_4. It shows that heating time has significant influence on the yield of AC. For example, AC8 achieved heights surface area for 60 min heating with lowest yield (66 %). On the other hand, due to decrease heating time 60–30 min, AC6 provided 75 % yield where other parameters are same as AC8.

Optimization of the activation process

In order to examine the main factors and their interactions for the surface area development of FAC, a factorial of the type 2^3 design was used. The regression analysis was performed to fit the experimental data. Design-Expert version 8 software package was used in this case. The main and interaction effects of each parameter for the development of surface area were analyzed and listed in Table 4. In this case, it can be seen that all main factors and their interactions have positive effects on surface area development, except BC and ABC, which have a negative effect. Among the parameters, temperature has the highest effects (about 46 % contributions) in surface area development followed by the heating time (24 % contributions). Based on effects analysis, a regression model (Eq. 7) was developed by coded factors to predict surface area development of unburned carbon derived from HOFA.

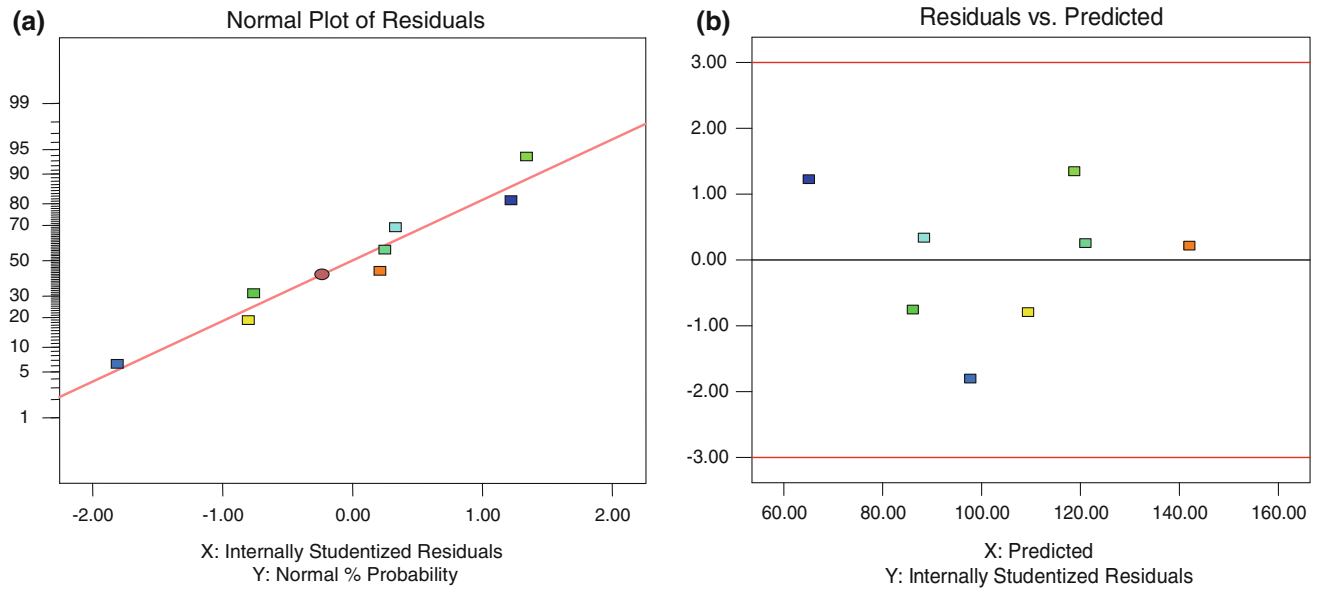

Fig. 7 **a** Normal probability plot of residuals, **b** residuals versus predicted plot

$$\text{Surface area} = 103.63 + 16.32 \times A + 11.64 \times B + 10.51 \times C + 1.94 \times AB + 6.51 \times AC - 2.45 \times BC - 4.22 \times ABC \quad (7)$$

It should be noted that the model parameters (Eq. 7) were determined by an analysis of variance (ANOVA) exercise so that the model could adequately correlate most of the data. In this case, A and B were found to be significant model terms. Considering the significant terms, the model presented a high determination coefficient ($R^2 = 0.8798$) claiming 87.98 % of the variation in surface area development can be explained by the independent variables: temperature, time and amount of H_3PO_4. Table 5 shows the experimental and predicted values of surface area development (based on main factors). Since the differences between the experimental and calculated are minimal, it can be said that the regression analysis is adequate. The normal probability plot of residuals (Fig. 7a) shows that the residual distribution is approximately normal, and there is no abnormality in the data set. Figure 7b shows the residuals versus predicted plot. The general impression from examining this figure is that the residual distribution is approximately constant variance. These diagnostic tests prove that the regression equation for surface area development is satisfactory.

In order to determine the optimum values and the limit of each independent variable, 3D response surface plots of the regression equation were generated. Figure 8a shows the interaction of temperature and heating effects on surface area development. It can be seen that both have the positive effects on final output. At maximum set condition, temperature has more influence on surface area development than heating time. Similarly, if we compare the interaction effect of temperature and H_3PO_4 (Fig. 8b), it shows both have positive effects, and the degree of influence of temperature is higher than H_3PO_4. Figure 8c instates the interaction effects of heating time and H_3PO_4 on surface area development, which have positive effects with almost equal degree of influence. By analyzing the 3D response surface plots, it is easy to evaluate the optimum values of the variables so that the response is maximized.

Each contour curve (bottom of the 3D surface diagram) represents an infinite number of combinations of two-test variables. It can be seen that the maximum predicted value is indicated by the surface confined into the smallest ellipse in the contour diagram. Elliptical contours are obtained when there is a perfect interaction between independent variables (Montgomery 1997). The surface plot in Fig. 8a

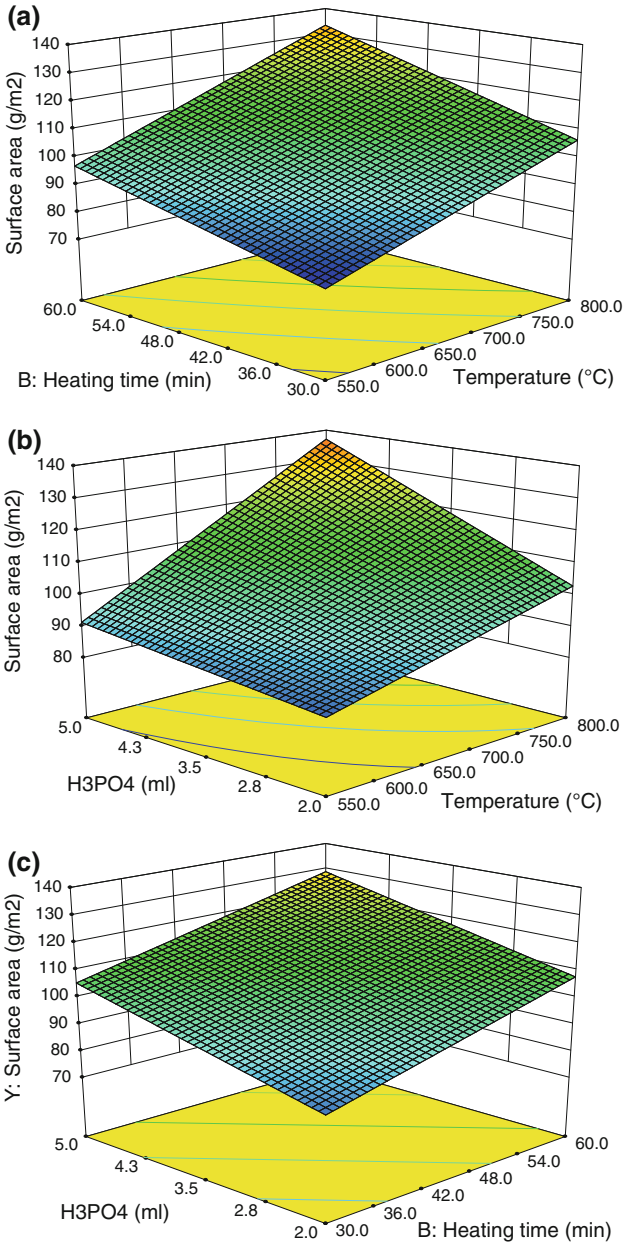

Fig. 8 **a** The interaction effect of heating time and temperature on surface area development. **b** The interaction effect of temperature and H_3PO_4 on surface area development. **c** The interaction effect of heating time and H_3PO_4 on surface area development

indicated that as the temperature and time increased, the development of surface area increased. Similar patterns were observed in Fig. 8b, c. However, it has been reported that high temperature may cause shrinkage of activated carbon at postsoftening and swelling, which results in narrow or close pores in the surface (Guo and Lua 1998). The higher temperature and holding time also reduced the percentage yield of FAC (Table 2). Thus, increasing

temperature higher than 800 °C may not be feasible for chemical activation of HOFA.

Conclusion

In this study, HOFA was used as a raw material for AC production. H_3PO_4 is used as a chemical agent to improve the surface characteristics of HOFA. Two-level factorial design is used to optimize the experimental process. Following the activation in presence of air, an optimal BET surface area of 144.88 m^2/g and pore volume 0.333 cm^3/g was obtained. The N_2-77 K adsorption isotherms show that the produced AC is mainly mesopores type with an estimated average pore size ranging between 4.51 and 8.19 nm. Based on the analysis, it can be concluded that Saudi Arabian HOFA can be used as an effective and inexpensive raw material for AC production, which has potential for various industrial application, especially in adsorption process for removal of pollutants with large molecules where a mesopore volume is required.

Acknowledgments Financial support provided by the Natural Sciences and Engineering Research Council (NSERC) of Canada is highly appreciated.

References

Ahmadpour A, Do DD (1996) The preparation of active carbons from coal by chemical and physical activation. Carbon 27(4):471–479

Brunauer S, Deming L, Deming W, Teller E (1940) On a theory of the van der Waals adsorption of gases. J Am Chem Soc 62(7):1723–1732

Caramuscio P, De Stefano L, Seggiani M, Vitolo S, Narducci P (2003) Preparation of activated carbons from heavy-oil fly ashes. Waste Manag 23:345–351

Cuhadaroglu D, Uygun OA (2008) Production and characterization of activated carbon from a bituminous coal by chemical activation. Afr J Biotechnol 7(20):3703–3710

Davini P (2002) Flue gas treatment by activated carbon obtained from oil-fired fly ash. Carbon 40:1973–1979

Fernandez A, Wendt JOL, Wolski N, Hein KRG, Wang S, Witten ML (2003) Inhalation health effects of fine particles from the co-combustion of coal and refuse derived fuel. Chemosphere 51:1129–1137

Ghio AJ, Silbajoris R, Carson JL, Samet JM (2002) Biologic effects of oil fly ash. Environ Health Perspectives, vol 110 Supplement 1, February

Gregg SJ, Sing KSW (1982) Adsorption, surface area and porosity. Academic Press, London, p 219

Guo J, Lua AC (1998) Characterization of chars pyrolyzed from oil palm stone for the preparation of activated carbons. J Anal Appl Pyrol 46:113–125

Hsieh YM, Tsai MS (2003) Physical and chemical analyses of unburned carbon from oil-fired fly ash. Carbon 41:2317–2324

Hwang SK, Park JH, Hong SU, Jung JH, Jung MY, Son YU, Cho KJ (1996) Engineering development and operation for heavy oil fly ash incineration plant, KEPRI-93C-T04. Korea Electric Power Research Institute, Korea

Jiang N, Dreher KL, Dye JA, Li Y, Richards JH, Martin LD, Adler KB (2000) Residual oil fly ash induces cytotoxicity and mucin secretion by guinea pig tracheal epithelial cells via an oxidant-mediated mechanism. Toxicol Appl Pharmacol 163:221–230

Kaneko N, Akahoshi T, Sakuma A, Ohyama H, Iijima M (1992) Recovery of valuables from oil fly ash. Chem Eng (Japan) 56(6):389–391

Kruk M, Jaroniec M (2001) Gas adsorption characterization of ordered organic-inorganic nanocomposite materials. Chem Mater 13(10):3181

Kwon WT, Kim DH, Kim YP (2005). Characterization of heavy oil fly ash generated from a power plant. doi:10.2240/azojomo0135

Lozano LJ, Juan D (2001) Solvent extraction of polyvanadates from sulphate solutions by primene 81R. Its application to the recovery of vanadium from spent sulphuric acid catalysts leaching solutions. Solvent Extr Ion Exch 19:659–676

Mofarrah A, Husain T, Danish EY (2011) Investigation of the potential use of heavy oil fly ash as stabilized fill material for construction. J Mater Civ Eng. doi:10.1061/(ASCE)MT.1943-5533.0000442 (9 December 2011

Mohapatra R, Rao JR (2001) Some aspects of characterisation, utilisation and environmental effects of fly ash. J Chem Technol Biotechnol 76:9–26

Montgomery DC (1997) Design and analysis of experiments, 4th edn. John Wiley and Sons Editions, New York

Mõtlep R, Sild T, Puura E, Kirsimäe K (2010) Composition, diagenetic transformation and alkalinity potential of oil shale ash sediments. J Hazard Mater 184(1–3):567–573

Onundi YB, Mamun AA, Al Khatib MF, AlSaadi MA, Suleyman AM (2011) Heavy metals removal from synthetic wastewater by a novel nano-size composite adsorbent. Int J Environ Sci Tech 8(4):799–806

Otterturn H, Standell E (1979) Solvent extraction of vanadium (IV) with di (2-ethyl-hexyl) phosphoric acid and tributylphosphate. CIM 21:501–508

Peter L (2008) In: Mota JP, Lyubchik S (eds) Recent advances in adsorption processes for environmental protection and security, pp 19–28

Rahman MA, Asadullah M, Haque MM, Motin MA, Sultan MB, Azad MAK (2006) Preparation and characterization of activated charcoal as an adsorbent. J Surface Sci Technol 22(3–4): 133–140

Rodríguez-Reinoso F, Linares-Solano A (1989) Chemistry and physics of carbon. In: Thrower PA (ed) vol 21, Marcel Dekker, New York, pp 1–146

Rouquerol F, Rouquerol J, Sing K (1999) Adsorption by powders and porous solids. Academic Press, San Diego

Sing KSW, Everett DH, Haul RAW, Moscou L, Pierotti RA, Rouquerol J, Siemieniewska T (1985) Reporting physisorption data for gas/solid systems with special reference to the determination of surface area and porosity (recommendations 1984). Pure Appl Chem 57(4):603–619

Singh BP, Besra L, Bhattacharjee S (2002) Factorial design of experiments on the effect of surface charges on stability of aqueous colloidal ceramic suspension. Colloid Surface 204(1–3):175–181

Soylak M, Narin İ, de Bezerra Almeida M, Ferreira SLC (2005) Factorial design in the optimization of preconcentration procedure for lead determination by FAAS. Talanta 65(4):895–899

Tsai SL, Tsai MS (1997) Study on the physical and chemical characteristics, yield and TCLP test of oil-fired fly ash. Mining Metall 41(2):57–68

Turner CW, Steve D (2009) Energy management handbook, 7th edn. The Fairmont Press, Inc., Lilburn, Georgia

Wesche K, Alonso IL, Bijen I, Schubert P, Vom Berg W, Rankers R (1989) Test methods for determining the properties of fly ash and

of fly ash for use in building materials. Mater Struct/Matdriaux et Constr 22:299–308

Wigmans T (1989) Industrial aspects of production and use of activated carbons. Carbon 27(1):13–22

Zhang P, Inoue K, Tsuyama H (1995) Recovery of metal values from spent hydrodesulfurization catalysts by liquid–liquid extraction. Energy Fuels 9(1995):231–239